Rock and Soil Mechanics

Volume 41 | Issue 9 Article 1

1-25-2021

# Dynamic triaxial test analysis of reinforced gravel soil under cyclic loading

Jia-quan WANG
*College of Civil Engineering and Architecture, Guangxi University of Science and Technology, Liuzhou, Guangxi 545006, China*

Zhen-chao CHANG
*Guangxi Beitou Transportation Maintenance Technology Group Co., Ltd, Nanning, Guangxi 530028, China*

Yi TANG
*College of Civil Engineering and Architecture, Guangxi University of Science and Technology, Liuzhou, Guangxi 545006, China*

Ying TANG
*College of Civil Engineering and Architecture, Guangxi University of Science and Technology, Liuzhou, Guangxi 545006, China*



## Custom Citation

WANG Jia-quan, CHANG Zhen-chao, TANG Yi, TANG Ying, . Dynamic triaxial test analysis of reinforced gravel soil under cyclic loading[J]. Rock and Soil Mechanics, 2020, 41(9): 2851-2860.

Rock and Soil Mechanics 2020 41(9): 2851−2860 ISSN 1000−7598
https: //doi.org/10.16285/j.rsm.2019.6977 rocksoilmech.researchcommons.org/journal

# Dynamic triaxial test analysis of reinforced gravel soil under cyclic loading

WANG Jia-quan[1], CHANG Zhen-chao[1, 2], TANG Yi[1], TANG Ying[1]
1. College of Civil Engineering and Architecture, Guangxi University of Science and Technology, Liuzhou, Guangxi 545006, China
2. Guangxi Beitou Transportation Maintenance Technology Group Co., Ltd, Nanning, Guangxi 530028, China

**Abstract:** In order to investigate the dynamic characteristics of reinforced gravel soil under cyclic loading, the consolidated undrained dynamic triaxial tests were carried out on the reinforced gravel soil with different numbers of reinforcement layers and confining pressures. The effects of the number of reinforcement layers and confining pressure on the dynamic characteristics of reinforced gravel soil were studied, and the development mechanism of axial cumulative strain of reinforced gravel soil was further analyzed. The results show that when the number of reinforced layers increases, the axial cumulative strain decreases, the rebound modulus increases, and the influence of reinforcement gradually decreases; when the confining pressure is increased, the axial cumulative strain of the soil decreases, and the rebound modulus and the dynamic pore pressure increase accordingly. As the number of reinforced layers and the number of cycle increase, the hysteresis curve gradually approaches the stress axis, and the hysteresis loop area gradually decreases, and the energy consumption of the soil weakens. Based on the stability theory and the indirect influence band theory, the mechanism of the influence of reinforcement on the development of axial cumulative strain is revealed. An axial cumulative strain prediction model of reinforced gravel soil that accounts for the effect of number of reinforcement layers is established. The parameters $\alpha$, $\beta$, $\gamma$ are linear with the number of reinforcement layers, and the model can effectively predict the deformation of reinforced gravel subgrade under cyclic loading.

**Keywords:** gravel soil; dynamic triaxial test; reinforced soil; dynamic characteristics; axial cumulative strain

## 1 Introduction

In recent years, geosynthetic reinforced soil technology has been widely used in many fields such as hydraulic projects, transportation, construction, and port because of its advantages in reducing the lateral deformation and vertical settlement, and in improving the bearing capacity and stability[1]. Gravel soil is a general designation of gravel, gravelly sand, silty gravel, and sandy gravel[2]. This type of soil has good mechanical performance and high permeability, and has been widely used in subgrade engineering. Compared with fine-grained soil, research on the dynamic characteristics of gravel soil is relatively rare, and the relevant theory is not thorough.

At present, scholars have conducted in-depth research on the static characteristics of gravel soil[3−4], and also have obtained some results on the dynamic characteristics. When the dynamic stress amplitude is low, the curves of accumulated axial strain versus number of loading cycles are stable, which show the law of hyperbolic function. In addition, the curves exhibit failure type and show the increasing rule in the form of the power function under the large dynamic stress amplitude[5−6]. Meanwhile, the axial accumulated strain decreases with increasing confining pressure, and increases with increasing dynamic stress amplitude and increasing number of cycles[7−8]. In term of the influence of frequency on the deformation characteristics of gravelly soil, Sun et al.[9] and Indraratna et al.[10] found that the axial strain development mode is plastic stable under small frequency, and the axial strain development mode is plastic failure under high frequency. The permanent deformation and deterioration of soil increase with increasing frequency. The rebound characteristics of gravel soil are also affected by confining pressure, number of cycles and dynamic stress amplitude. In addition, the rebound modulus increases gradually with the increase of confining pressure and number of cycles[11−12].

Aforementioned previous studies are experimental studies on the dynamic characteristics of unreinforced gravel soil. With the development of geosynthetics, the application of geosynthetic reinforced soil(GRS) in engineering practice is becoming more and more extensive, and the relevant experimental studies have also been carried out. Latha et al.[13] conducted the dynamic triaxial tests on reinforced sand and found the dynamic modulus does not change with the increase of reinforcement layers under the low confining pressure. However, as the reinforcement layers increase, the dynamic modulus increases significantly under the high confining pressure. Moayed et al.[14] found the laying position of the geotextile layers plays an important role in the dynamic characteristics through the dynamic triaxial test of reinforced sand,

Received: 20 November 2019 Revised: 19 March 2020
This work was supported by the Natural Science Foundation of China(41962017), the Natural Science Foundation of Guangxi Province of China (2017GXNSFAA198170), the High Level Innovation Team and Outstanding Scholars Program of Guangxi Institutions of Higher Learning, China, Graduate Student Education Innovation Projects of Guangxi University of Science and Technology(GKYC201907) and Guangxi College Students Innovation and Entrepreneurship Training Program(201910594190).
First author: WANG Jia-quan, male, born in 1981, PhD, Professor, mainly engaged in teaching and research on reinforced soil structures and foundation engineering. E-mail: wjquan1999@163.com

and its liquefaction resistance can be improved when the position of geotextile approaches the top of the sample. Wang et al.[15] found that the dynamic pore pressure of reinforced gravel soil increases with the increase of confining pressure under the same dynamic stress, but the pore pressure ratio is essentially about 0.5.

In summary, scholars have studied the dynamic characteristics of unreinforced gravel soils under different confining pressures, dynamic stress amplitudes, frequencies and so on. For geosynthetic reinforced soils, some scholars have analyzed the dynamic characteristics of reinforced soils in terms of reinforcing modes and the number of reinforcement layers. However, most of the research on reinforced soil focused on fine sand, clay or gravel, but there are few studies on the dynamic characteristics of reinforced gravel soil. Therefore, in this paper the biaxial geogrid is used as the reinforced material for dynamic triaxial tests of reinforced gravel soil. By studying the influence of confining pressure and the number of reinforcement layers on the dynamic characteristics, such as axial cumulative strain, rebound modulus, dynamic pore pressure, etc., and the development mechanism of axial cumulative strain of reinforced gravel soil are analyzed. This study aims to provide useful guidance for controlling and reducing the settlement of reinforced subgrade.

## 2 Test setup and scheme

### 2.1 Testing apparatus

The test adopted GDS dynamic triaxial testing system, consisting of drive motor, pressure chamber, load sensor, pore pressure sensor, DCS data acquisition control box, confining pressure/back pressure control system, GDSLAB data acquisition and control program and other modules. The basic technical indexes are as follows: maximum axial dynamic load of 10 kN, maximum confining pressure of 2 MPa, dynamic loading frequency range of 0−5 Hz, and the applied waveforms of sine wave, half sine wave, triangular wave and square wave, etc.

### 2.2 Test material

The test soil sample was taken from a river embankment in Liuzhou, Guangxi. According to the grain-size analysis, the coefficients of uniformity and curvature of sample are $C_u = 5$ and $C_c = 1.25$, respectively, which indicates that this is a well-graded sand. The corresponding gradation curve is shown in Fig.1. The specific gravity of gravelly sand is 2.67, the maximum dry density is 1.81 g/cm$^3$, the minimum dry density is 1.56 g/cm$^3$, the controlled dry density is 1.77 g/cm$^3$, and its relative density is 0.86. The reinforcement material used in the test is biaxial geogrid, the aperture size of which is 20 mm × 20 mm. The transverse tensile yield force is 15.4 kN/m, and the longitudinal tensile yield force is 18.6 kN/m.

### 2.3 Testing Scheme

This test is a large-size consolidated undrained dynamic triaxial test. As shown in Fig. 2, the cylindrical sample has a diameter of 150 mm and a height of 300 mm. The ratio of height to diameter $H/D$ is 2.0, and the reinforcement is arranged at equal vertical spacing. The sample is saturated with carbon dioxide saturation and water saturation firstly, and then the method of back pressure saturation is adopted. When the pore water pressure coefficient $B$ satisfies $B \geqslant 0.96$, the sample is considered to be fully saturated. Based on the calculation method of frequency $f = V/L$ proposed by Liu et al.[16], the speed $V$ = 72 km/h, length of single carriage $L$ = 20 m, and the frequency $f$ = 1 Hz were used for the test. According to the research by Huang et al.[17] on the simulation of high-speed train loading using dynamic triaxial test, the half sine wave was selected as the cyclic loading waveform. The influence of the number of reinforcement layers on the dynamic characteristics with confining pressure of 90 kPa and dynamic stress amplitude of 135 kPa, and the influence of confining pressure on the dynamic characteristics with dynamic stress amplitude of 90 kPa and three layers of reinforcement were investigated, respectively. The evolution law of hysteretic curve of reinforced gravel soil with different number of reinforced layers was also analyzed. The testing parameters are shown in Table 1.

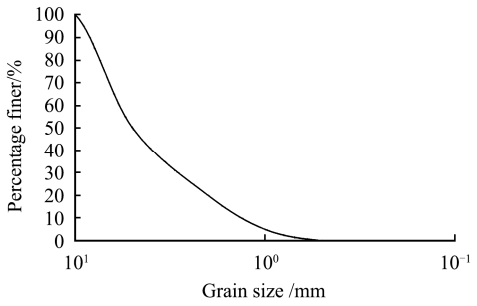


**Fig. 1 Grain-size distribution curve of sand samples**

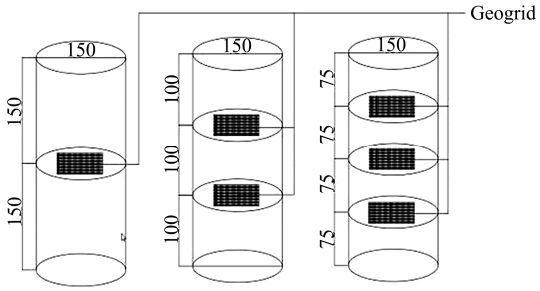


(a) 1-layer reinforcement (b) 2-layer reinforcement (c) 3-layer reinforcement

**Fig. 2 Schematic diagram of geogrid laying(unit: m)**

**Table 1 Testing parameters**

| Type | Confining pressure /kPa | Dynamic stress amplitude /kPa | Reinforcement layer |
|---|---|---|---|
| A-1-1 | 60 | 90 | 3 |
| B-1-1 | 90 | 90 | 3 |
| B-2-1 | 90 | 135 | 0 |
| B-2-2 | 90 | 135 | 1 |
| B-2-3 | 90 | 135 | 2 |
| B-2-4 | 90 | 135 | 3 |
| C-1-1 | 120 | 90 | 3 |

### 2.4 Testing procedures

The testing process is basically similar under various working conditions, and the main procedure can be divided into six steps: (1) The sand samples collected from the site were sieved. (2) The sand sample was compacted with six layers, and the same density was ensured by controlling the number of compaction and compaction quality. (3) The pressure chamber was closed after installing the sample, then the pressure chamber was filled with water. (4) The sample was ensured to be fully saturated. (5) The isotropic consolidation mode with the consolidation ratio $K$c = 1.0 was used to consolidate the samples. (6) After the consolidation was completed, the cyclic loading was applied, and the specific dynamic parameters were determined according to the test condition.

The test was stopped either when the axial cumulative strain reached 5% or the number of cycles was 5 000. The number of points for measurement during each cycle was set to 20, meaning 20 data points were recorded per second under the frequency of 1 Hz. The changes of axial dynamic stress, dynamic strain and dynamic pore pressure were monitored and collected in real time by GDSLAB data acquisition system and control program.

## 3 Analysis of test results

### 3.1 The influence of number of reinforcement layers on the dynamic characteristics of reinforced gravel soil

3.1.1 The influence on axial cumulative strain

In order to better evaluate the influence of reinforcement on the axial cumulative strain and rebound modulus, the following reinforcing coefficients $R_{\varepsilon d}$ and $R_{Ed}$ are introduced by referring to the study of Wang et al.[18]

$$R_{\varepsilon d} = \frac{\varepsilon_{d0} - \varepsilon_{di}}{\varepsilon_{d0}} \quad (1)$$

$$R_{Ed} = \frac{E_{di} - E_{d0}}{E_{d0}} \quad (2)$$

where $R_{\varepsilon d}$ is the reinforcing coefficient of axial cumulative strain; $\varepsilon_{d0} - \varepsilon_{di}$ is the final difference of axial cumulative strain between $i$ layer of reinforcement and nonreinforcement; $\varepsilon_{d0}$ is the final axial cumulative strain of nonreinforcement; $R_{Ed}$ is the reinforcing coefficient of rebound modulus, $E_{di} - E_{d0}$ is the final difference of rebound modulus between $i$ layer of reinforcement and nonreinforcement; and $E_{d0}$ is the final rebound modulus of nonreinforcement.

As shown in Fig.3, the $\varepsilon_d - N$ ($N$ is the number of cycles) curve is plotted from top to bottom with the increase of reinforcement layers, which indicates that the axial cumulative strain decreases with the increase of reinforcement layers. It can be seen from Table 2 that $R_{\varepsilon d}$ of reinforced samples is positive, which means that the reinforcement in each layer can reduce the axial cumulative strain. As the number of reinforcement layers increase, $R_{\varepsilon d}$ gradually increases, and $R_{\varepsilon d}$ = 0.522 when three layers are reinforced. Compared with the unreinforced sample, the results show the axial cumulative strain with three layers of reinforcement is reduced by about a half. As the number of reinforcement layers increases, the reinforcing effect enhances, the increments of $R_{\varepsilon d}$ are 0.324, 0.121 and 0.077, respectively, showing a decreasing trend, which indicates that the influence of reinforcement on the axial cumulative strain gradually decreases. Combined with the theory of indirect influence zone[19], the position of the soil particles near the reinforcement will rearrange during cyclic loading, which will enhance the strength and stiffness, and improve the resistance to deformation. Therefore, the development of cumulative strain will be reduced. The indirect influence band expands with the increase of reinforcement layers, which enlarges the strengthening area of the sample, and the reinforcing effect is more significant. However, the indirect influence bands will be superimposed on each other when the number of reinforcement layers increase to a certain value, and the reinforcing effect will be affected. It shows that the influence of reinforcement on axial cumulative strain gradually decreases with the increase of reinforcement layers.

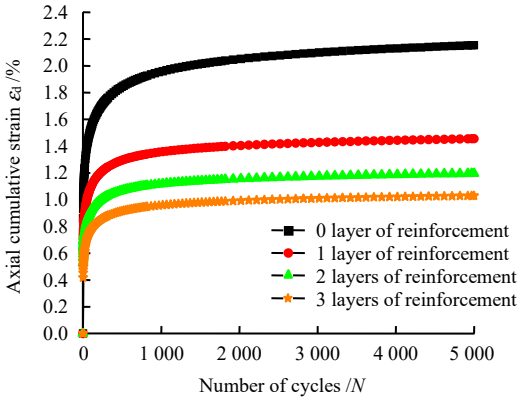


**Fig. 3 Curves of cumulated axial strain with the number of loading cycles**

**Table 2 Reinforcing coefficients for different number of reinforcement layers**

| Reinforcement layer $\lambda$ | $R_{\varepsilon d}$ | $R_{Ed}$ |
|---|---|---|
| 0 layer | 0.000 | 0.000 0 |
| 1 layer | 0.324 | 0.064 3 |
| 2 layers | 0.445 | 0.075 6 |
| 3 layers | 0.522 | 0.086 8 |

Referring to the research by Ma et al.[5] on axial cumulative strain of saturated gravels and using the hyperbolic model proposed by them to model the relationship between the axial cumulative strain and the number of cycles, it is found that the relationship between the axial cumulative strain and the number of cycles does not conform to the hyperbolic model. It shows the relationship

between axial cumulative strain and the number of cycles is affected by the types of soil, and the relations for different types of soil are different. Therefore the hyperbolic model cannot be applied directly.

Consequently, the relationship between axial cumulative strain and the number of cycles of reinforced gravel soil is refitted and analyzed by MATLAB software, and the prediction model for reinforced gravel soils with different number of reinforcement layers is established as:

$$\varepsilon_d = \frac{N}{\alpha + \beta N + \gamma N^{0.5}} \quad (3)$$

where $\varepsilon_d$ is the axial cumulative strain; and $\alpha$, $\beta$, $\gamma$ are the fitting parameters related to the number of reinforcement layers.

The values of the fitting parameters $\alpha$, $\beta$, and $\gamma$ are given in Table 3. After the fitting analysis, it is found the relationship between fitting parameters $\alpha$, $\beta$, $\gamma$ and the number of reinforcement layers $\lambda$ are linear. As shown in Fig.4, the parameter $\alpha$ decreases linearly with the increase of reinforcement layers, while the parameters $\beta$ and $\gamma$ increase linearly. The equations describing the relationship between the number of reinforcement layers and the fitting parameters are summarized as follows:

$$\alpha = -0.311\lambda - 1.488 \quad (4)$$

$$\beta = 0.16\lambda + 0.47 \quad (5)$$

$$\gamma = 0.525\lambda + 2.016 \quad (6)$$

**Table 3 Parameters and determination coefficients for different number of reinforcement layers**

| Reinforcement layer $\lambda$ | Fitting parameters | | | Determination coefficient |
|---|---|---|---|---|
| | $\alpha$ | $\beta$ | $\gamma$ | $R^2$ |
| 0 layer | −1.527 | 0.445 | 2.075 | 0.990 |
| 1 layer | −1.786 | 0.660 | 2.533 | 0.994 |
| 2 layers | −2.017 | 0.805 | 2.907 | 0.995 |
| 3 layers | −2.485 | 0.929 | 3.700 | 0.997 |

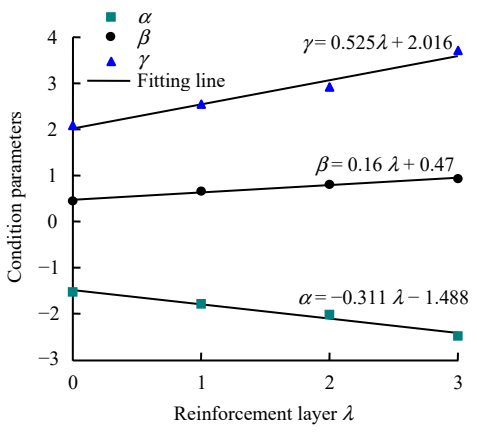


**Fig. 4 Relationships between parameters and the number of reinforcement layers**

Based on the linear relationship between the number of reinforcement layers and the fitting parameters, the fitting parameters corresponding to different reinforcement layers can be obtained by the above equations, and then the axial cumulative strain of reinforced gravels soils with different reinforcement layers can be predicted by the prediction model.

As shown in Fig.5, the predicted values of axial cumulative strain with different reinforcement layers are basically consistent with the measured values, and the corresponding determination coefficient of the prediction model under each reinforcement layer is greater than 0.99. It can be seen that the prediction law of the axial cumulative strain model is consistent with the experimental results, which shows the prediction model is reasonable. Meanwhile, the prediction model and condition parameters can provide a reference for predicting the cumulative deformation of reinforced gravel soil under cyclic loading.

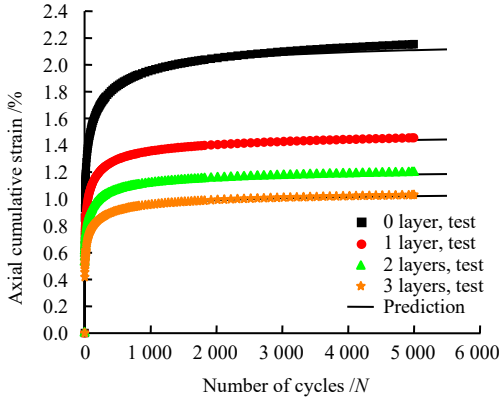


**Fig. 5 Axial cumulative strains and the number of cycles for different number of reinforcement layers**

3.1.2 The influence on rebound modulus

Figure 6 shows the relationship between rebound modulus $E_d$ and the number of cycles $N$ under different reinforcement layers. The rebound modulus shows the development trend of slight decrease–increase–stable with the continuous application of dynamic loading. The spacing of curves gradually decreases when the number of reinforcement layers increases. It can be seen from Table 2 that $R_{Ed}$ increases from 0.064 3 to 0.086 8 with the increase of number of reinforcement layers, which indicates that the lateral deformation of soils is limited and the overall stiffness is improved. Finally, the rebound modulus increases.

Comparing $R_{Ed}$ between adjacent reinforcement layers in Table 2, it is found the differences of $R_{Ed}$ between adjacent reinforcement layers are 0.064 3, 0.011 3 and 0.011 2, respectively, and the difference between the unreinforced case and the case with 1 layer of reinforcement is the largest. At the same time, the influence of reinforcement on rebound modulus will gradually decrease with the increase of reinforcement layers. By analyzing the initial position of the curve in Fig.6, it is found that

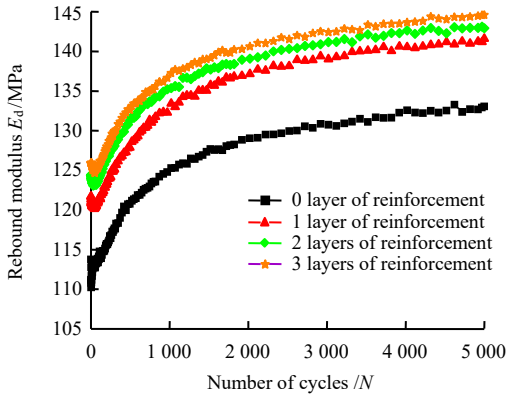


**Fig. 6 Relationships between rebound modulus and the number of cycles for different number of reinforcement layers**

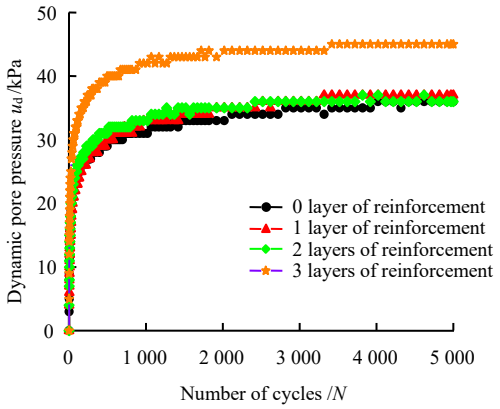


**Fig. 7 Curves of dynamic pore water pressure and the number of cycles for different number of reinforcement layer**

the reinforcement not only affects the rebound modulus during cyclic loading, but also has a significant impact on the initial rebound modulus, and the initial value of the rebound modulus increases with the increase of reinforcement layers. It indicates that the reinforcement can improve the overall stiffness, and the increase in the number of reinforced layers will weaken the impact on the rebound modulus. The reason for this situation is that the increase in the number of reinforced layers causes the indirect influence zones to overlap each other, which interferes with the interaction of the reinforcement and soil, resulting in the gradual weakening of the increase in the elastic modulus of the reinforcement. Therefore, reinforcement can improve the overall stiffness of the subgrade soil, and reduce the settlement of subgrade under cyclic loading. However, it is necessary to determine the appropriate reinforcement layers to reduce the waste of reinforcement materials and to improve economic benefits.

3.1.3 The influence on dynamic pore pressure

As shown in Fig.7, the curves of dynamic pore water pressure and the number of cycles for different number of reinforcement layers are basically in the same shape and follow a pattern of steady growth. The dynamic pore pressure has a leap-growth for three layers of reinforcement, which indicates that the three layers of reinforcement have a significant influence on the dynamic pore pressure. Adopting one and two layers of reinforcement has a small effect on the dynamic pore pressure. It is worth mentioning that the increase of dynamic pore pressure is not the real situation due to the embedding effect induced by the rubber film for the large diameter triaxial sample. However, as the reinforcing effect is determined relatively, the influence of rubber film embedding effect on the reinforcement effect can be ignored in this paper.

It can be seen from Fig.8 that the bulk shrinkage phenomenon occurs in the samples under cyclic loading, and the volumetric strain develops rapidly at the initial stage of loading, However, when the number of cycles $N = 200$, the growth rate of volumetric strain will gradually decrease. The results show that the reinforcing effect on the volumetric strain of the sample is small with one layer and two layers of reinforcement, and the volumetric strain is significantly increased with 3 layers of reinforcement. The soil becomes denser in the process of cyclic loading, which is not favorable to the dissipation of excess pore water pressure, resulting in the pore pressure level higher than with 0, 1, and 2 layers of reinforcement. It should be noted that the dynamic pore pressure of the sample jumps significantly when the number of reinforcement layers increases from 2 to 3. A similar phenomenon can also be observed for volumetric strain. When the number of reinforcement layers is less than three, the reinforcing effect on the volumetric strain of the sample is small, and the effect is significantly increased when the number of reinforcement layers is greater than or equal to three. The dynamic pore pressure also shows the same behavior due to the influence of the volumetric deformation of the sample. Therefore, it is necessary to consider the influence of number of reinforcement density on dynamic pore pressure. Meanwhile, the reinforcement density should be selected reasonably to avoid reducing the stability of the geotechnical structure.

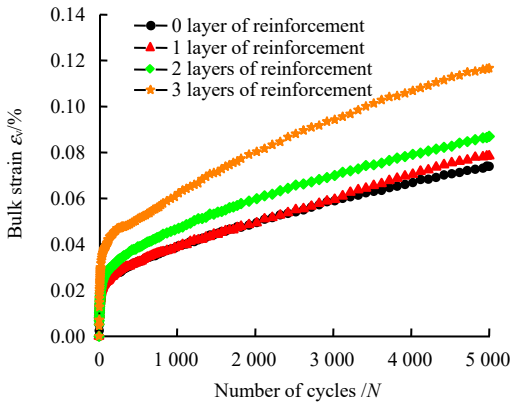


**Fig. 8 Relationships between volumetric strain and the number of cycles for different number of reinforcement layers**

### 3.2 The influence of confining pressure

3.2.1 The influence on axial cumulative strain

As shown in Fig.9, the $\varepsilon_d - N$ curves under confining pressure are similar to the $\varepsilon_d - N$ curves under different reinforcement layers, which shows a stable growth law. As the confining pressure increases, the $\varepsilon_d$ of reinforced gravelly soil will decrease, which is similar to the results of Liu et al.[20] It can also be found from Fig.9 that the spacing between curves increases with the increase of confining pressure. This is because the reinforcing effect of geogrid can be divided into two parts: the resistance provided by longitudinal and transverse ribs of geogrid, and the interlocking and sliding friction between the grid and the soil particles at the interface. When the confining pressure increases, the normal stress on the interface increases, which leads to an increase in friction and the effect of reinforcement and soil is enhanced. Meanwhile, the friction of soil particles can be increased by increasing the confining pressure, which then improves the strength and stiffness. The combined effect of increased strength and stiffness results in the reduction of axial cumulative strain.

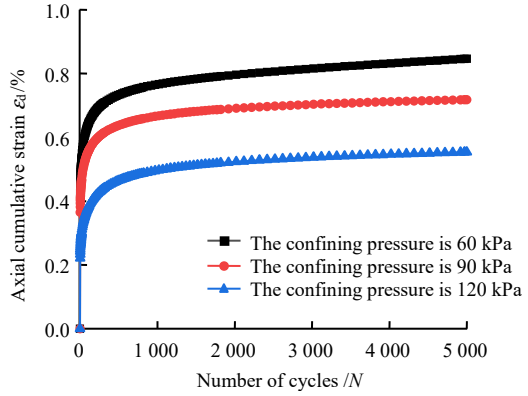


**Fig. 9 Axial cumulative strains and the number of cycles under different confining pressures**

By comparing the $\varepsilon_d$ after the first cyclic loading and the 5 000th cyclic loading in Table 4, it is found that about 50% of $\varepsilon_d$ is generated at the first cyclic loading. This is because the axial dynamic deviatoric stress is suddenly applied at the initial stage of cyclic loading, and the corresponding axial dynamic strain will increase rapidly. Meanwhile, the overall stiffness of soil is improved with the increase of confining pressure, and the $\varepsilon_d$ produced by the first cyclic loading under the same dynamic stress is reduced. Therefore, the increasing confining pressure can significantly inhibit the development of axial cumulative strain under the same dynamic stress.

**Table 4 Comparisons of axial cumulative strain under different confining pressures**

| Confining pressure /kPa | Cumulative strain / $\varepsilon_d$ % | |
|---|---|---|
| | $N$ = 1 | $N$ = 5 000 |
| 60 | 0.401 | 0.846 |
| 90 | 0.365 | 0.718 |
| 120 | 0.221 | 0.554 |

3.2.2 The influence on rebound modulus

It can be seen from Fig.10 that the development trend of rebound modulus under various confining pressures is similar to the trend of different reinforcement layers. The dynamic rebound modulus decreases rapidly at the initial stage of cyclic loading, then it increases gradually and tends to be stable. This law is due to the destruction of the original skeleton structure of the soil after the dynamic loading is applied, and then the sample will have a large deformation. The soil particles will rearrange, and subsequently reconstruct. During the rearrangement of soil particles, the soil status will gradually develop from the damaged state to a new stable state. Meanwhile, the soil particles tend to be denser, and the stiffness of soil increases. The rebound modulus will decrease to the lowest value, and then gradually increase and become stable.

According to the $E_d - N$ curve in Fig.10, it is found that the rebound modulus increases with the increase of confining pressure. However, when the increment of confining pressure is 30 kPa, the increase of rebound modulus under a high confining pressure is obviously smaller than that under a low confining pressure, which can be seen from the spacing between curves. It also reflects the influence of confining pressure on the rebound modulus decreases with the increase of confining pressure.

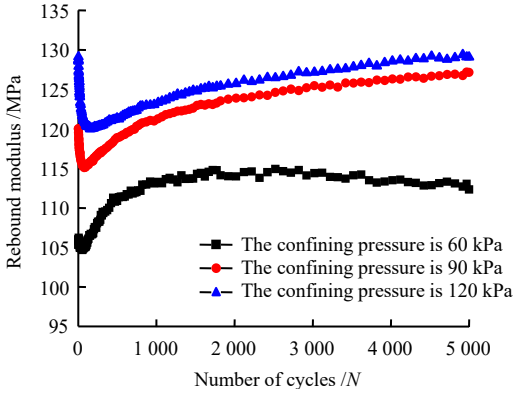


**Fig. 10 Relationships between rebound modulus and number of cycles under different confining pressures**

3.2.3 The influence on dynamic pore pressure

Figure 11 and Table 5 show the development law of dynamic pore pressure under different confining pressures. The development law of dynamic pore pressure with the number of cycles under various confining pressures is similar to that under different reinforcement layers, which shows a stable growth. As the confining pressure increases, the dynamic pore pressure increases, but the pore water pressure ratio (the ratio of dynamic pore water pressure $\sigma_d$ to confining pressure $\sigma_3$) remains basically constant.

However, the pore water pressure ratio can be used to represent the liquefaction level of the soil, and the soil liquefies when the pore water pressure ratio is 1.

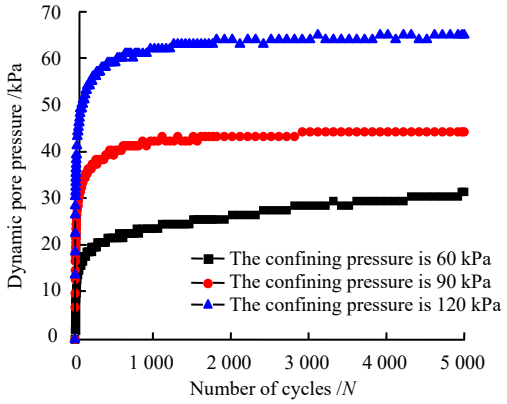


**Fig. 11 Curves of dynamic pore water pressure and the number of cycles under different confining pressures**

**Table 5 Pore water pressure ratios under different confining pressures**

| Confining pressure /kPa | Maximum dynamic pore pressure/kPa | Pore pressure ratio |
|---|---|---|
| 60 | 32 | 0.53 |
| 90 | 45 | 0.50 |
| 120 | 66 | 0.55 |

Based on the change of pore pressure ratio shown in Table 5, it can be found that confining pressure has a significant effect on dynamic pore pressure, but it has little effect on pore pressure ratio, and the level of liquefaction is less affected by the confining pressure. This is because the liquefaction level of soils mainly depends on the capacity of excess pore water pressure dissipation. In other words, the pore pressure is dissipated through the drainage boundary and the internal drainage condition. In this test, the boundary is undrained, and the compactness of the samples is the same. Therefore, the internal drainage conditions are basically the same, and the change of pore pressure ratio is small. The pore pressure ratio under different confining pressures remains around 0.5, which is far from the liquefaction pore pressure ratio. The results show that the reinforced gravelly soil has a good liquefaction resistance, and there are certain advantages when it is used as subgrade filler to resist traffic dynamic loading in subgrade engineering.

### 3.3 Analysis of hysteresis curves

The area of hysteretic curve can reflect the damping ratio and the energy dissipation effect of soils. The slope of hysteretic curve can reflect the rebound modulus of soils and describe the soil stiffness. Therefore, the evolution process of hysteresis curve can directly reflect the development law of rebound modulus and damping ratio.

#### 3.3.1 Hysteresis curves with different reinforcement layers

The hysteretic curves under different reinforcement layers are plotted in Fig.12. As the number of reinforcement layers increases, the hysteretic curve gradually

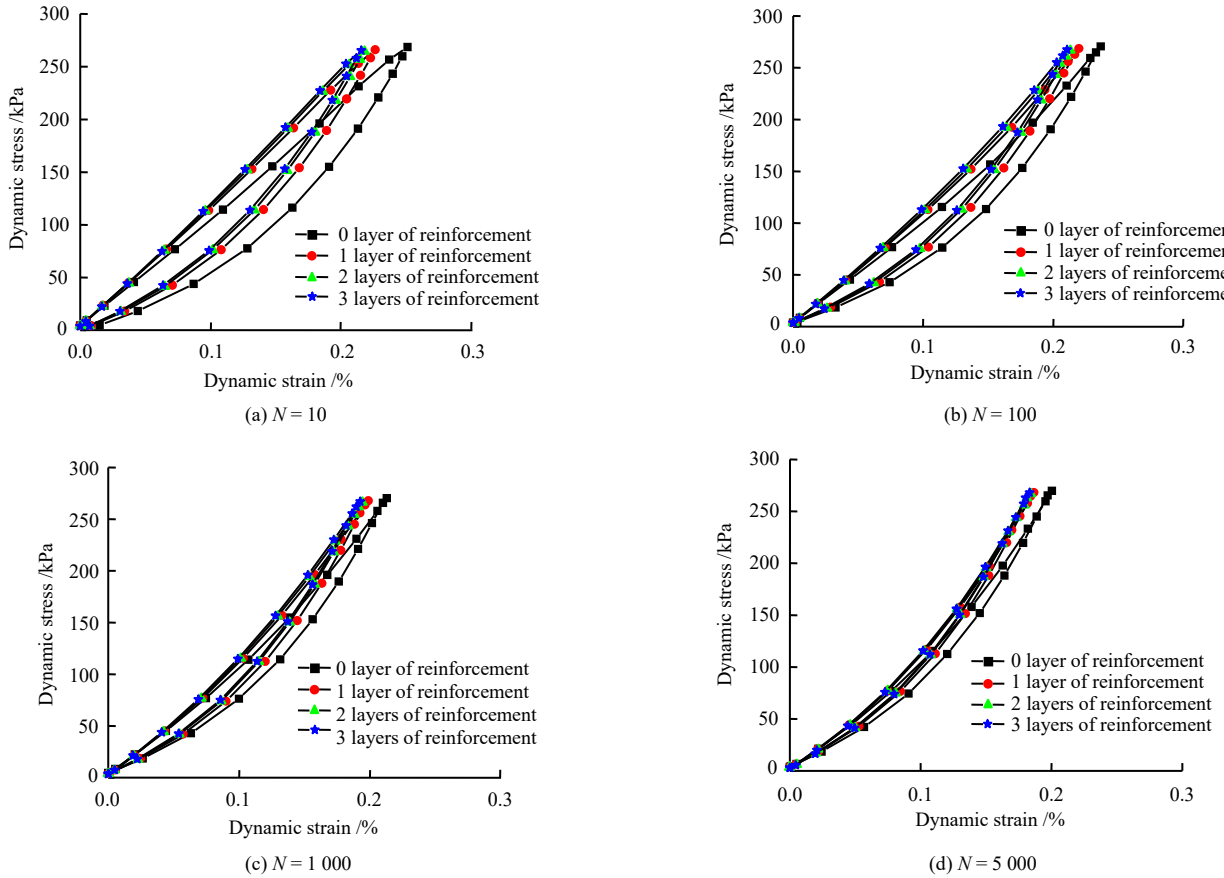


**Fig. 12 Stress−strain hysteresis curves for different number of reinforcement layers**

approaches the stress axis and the slope increases gradually. Moreover, the area of the hysteresis loop changes significantly under different reinforcement layers. The area of hysteresis loop gradually decreases with the increase of reinforcement layers. Especially for the case with number of cycles $N = 5\ 000$ and three layers of reinforcement, the hysteresis loop is almost linear.

As the number of cycles increases, the evolution process of hysteretic curve shows that the rebound modulus increases. However, the damping ratio decreases, which also reveals the law of rebound modulus in Fig. 6. In addition, the reduction in damping ratio will lead to the reduction in energy dissipation under traffic dynamic loading, which is not favorable to the seismic resistance of the soil.

It can be concluded that the reinforcement can improve the stiffness of soil and reduce the settlement of subgrade under traffic dynamic loading, but it is not favorable to the seismic resistance performance. Therefore, it is necessary to consider the appropriate reinforcement layers.

3.3.2 Hysteresis curves under different number of cycles

Figure 13 shows the evolution of the stress−strain hysteresis curves under different number of cycles for soil samples with different reinforcement layers. The area and slope of the hysteresis loop will change under different number of cycles. As the number of cycles increases, the area of the hysteresis loop will decrease, but the slope will gradually increase.

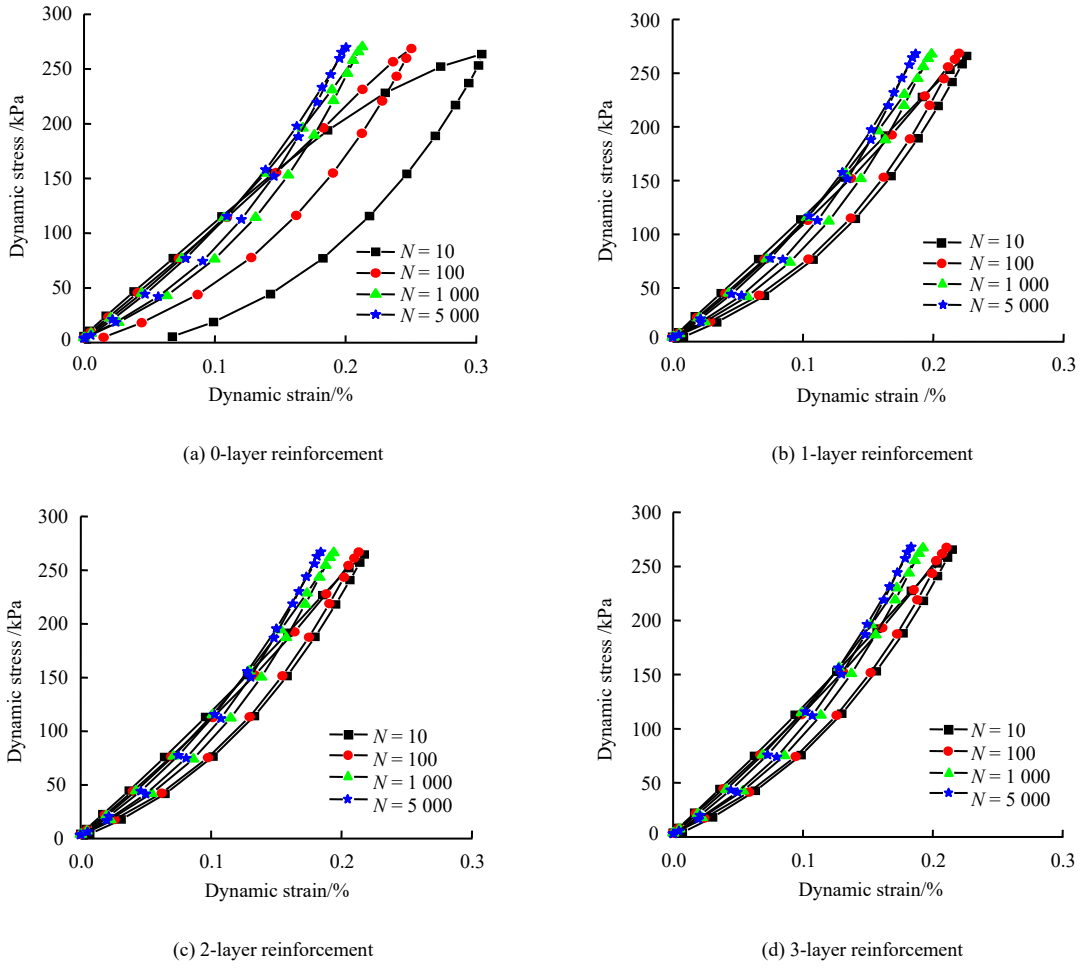


**Fig. 13 Stress−strain hysteresis curves under different number of cycles**

By comparing the hysteresis curves with different reinforced layers, it is found that the slope and area of nonreinforcement change significantly with the increase of cycles. As the number of cycles increases, the slope increases, the hysteretic curve gradually approaches the stress axis, and the rebound modulus of soil increases. In addition, the area of hysteresis loop decreases with the increase of cycles, the hysteresis loop tends to be linear gradually, and the damping ratio of soil decreases, showing obvious elastic response.

Comparing Figs.13(a), 13(b), 13(c) and 13(d), as the reinforced layer increases, it is found that the hysteresis loops gradually approach each other, the area decreases, and the energy dissipation of the soil gradually decreases. The hysteretic loops in Fig.13(a) are relatively scattered, while in Fig.13(d), the hysteresis loops tend to be closer. Especially, the hysteresis loops almost coincide when the number of cycles is between 1 000 and 5 000. It shows that reinforcement has a significant effect on restraining soil deformation and improving the soil resistance under

long-term cyclic loading.

### 3.4 Discussion on the mechanism of axial cumulative strain development

As for the development mechanism of axial cumulative strain of reinforced gravel soil, the effects of number of cycles and reinforcement layer are discussed in this paper, respectively.

Through the $\varepsilon_d - N$ curve in Fig.3, the development trend of axial cumulative strain under reinforcement layer is stable. As the number of cycles increases, the growth rate of the axial cumulative strain decreases and tends to be stable. Combined with the research by Wu et al.[21], it can be explained by shakedown theory that the strain behavior of reinforced soil under cyclic loading can be divided into four stages: pure elastic behavior, elastic shakedown behavior, plastic shakedown behavior and cumulative failure behavior. According to the hysteretic curve in Fig.14, the growth rate of $\varepsilon_d$ is larger at the initial stage of cyclic loading, and the hysteresis curve is not closed. It shows that plastic deformation is accumulated after the dynamic loading is applied. However, as the dynamic loading increases, the soil is gradually compacted, the resistance to deformation is enhanced, the growth rate of $\varepsilon_d$ gradually decreases within a limited number of cycles, and the elastic deformation of the soil is gradually reflected. In addition, the hysteresis curve becomes dense and gradually closed, and the soil axial cumulated strain reaches stable. During this process, part of the energy is absorbed by the soil, and only a small amount of plastic deformation is produced, which shows elastic response. Therefore, the deformation behavior of soil under this condition is considered as elastic shakedown behavior and plastic shakedown behavior.

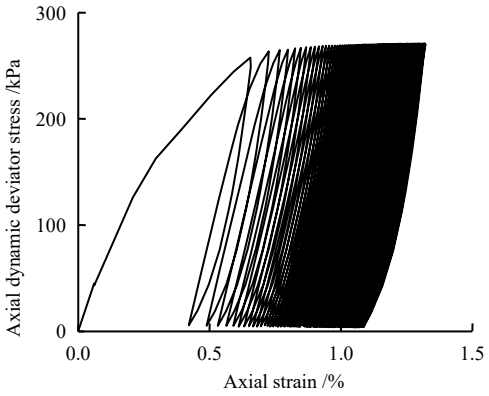


**Fig. 14 Hysteresis curve development mode of reinforced gravel soil**

As the number of reinforcement layers increases, the influence of reinforcement on $\varepsilon_d$ will gradually decrease, and the same law can be found in Fig.3. This law can be explained by the indirect influence band theory. When the reinforcement is placed in the soil, its indirect influence zone has a certain range. If the reinforcement spacing is small, the indirect influence band of reinforcement will be overlapped, and the interaction between reinforcement material and soil will be affected to a certain extent, which will reduce the reinforcing effect. Therefore, under the premise of satisfying bearing capacity and deformation requirement, the number of reinforcement layers should be reduced as much as possible in practical engineering, which can not only reduce the waste of reinforcement materials, but also improve economic benefits.

## 4 Conclusions

As the number of reinforcement layers increases, the axial cumulative strain decreases, and the rebound modulus increases. The reinforcing effect is gradually enhanced, and the increasing amplitude gradually decreases. The dynamic pore water pressure of the soil samples with one layer and two layers of reinforcement is close to that with zero layer of reinforcement, and the dynamic pore pressure with three layers of reinforcement increases significantly.

The development trend of axial cumulative strain and dynamic pore pressure are in line with the stable growth law. The prediction model for reinforced gravel soils is established, which can reflect the axial cumulative strain with different numbers of reinforced layers. The fitting parameter $\alpha, \beta, \gamma$ has a linear relationship with the number of reinforcement layers. Meanwhile, the model can effectively predict the cumulative settlement law of reinforced gravel subgrade under cyclic loading.

As the confining pressure increases, the axial cumulative strain of reinforced gravel soil decreases significantly, and the rebound modulus and dynamic pore pressure increase. However, the influence of confining pressure on the rebound modulus will attenuate as the confining pressure increases, and the influence on pore water pressure ratio is not obvious.

As the number of reinforcement layers and the number of cycles increase, the hysteresis loop area gradually decreases. This reflects that the rebound modulus of soil increases, the damping ratio decreases, and the energy consumption of the soil weakens. Therefore, it is not favorable to requirements of seismic resistance.

The development mechanism of axial cumulative strain $\varepsilon_d$ of reinforced gravel soil is obtained as follows: (i) As the number of cycles increases, $\varepsilon_d$ tends to be stable, and the plastic deformation is accumulated under dynamic loading. In addition, the growth rate of $\varepsilon_d$ gradually decreases and tends to be stable with the compaction of soil. (ii) As the number of reinforcement layers increases, the reinforcing effect on $\varepsilon_d$ decreases, and it is easy to weaken the reinforcing effect due to the superposition and interference of the indirect influence band.

## References

[1] PAN Hong-ke, ZHU Yan-zhi. Foundation treatment technology and foundation pit engineering[M]. Beijing: China Machine Press, 2015.

[2] YUAN Xiao-ming, QIN Zhi-guang, LIU Hui-da, et al. Necessary trigger conditions of liquefaction for gravelly soil layers[J]. Chinese Journal of Geotechnical Engineering, 2018, 40(5): 777−785.

[3] LI Xiao-gang, ZHU Chang-qi, CUI Xiang, et al. Experimental study of triaxial shear characteristics of carbonate mixed sand[J]. Rock and Soil Mechanics, 2020, 41(1): 123−131.

[4] WANG Qi-yun, ZHANG Jia-sheng, DENG Guo-dong, et al. Large-scale triaxial test study on shear dilatancy of subgrade filler of group B coarse-grained soil of high speed railway[J]. Journal of Railway Science and Engineering, 2015, 12(4): 731−736.

[5] MA Shao-kun, WANG Bo, LIU Ying, et al. Large-scale dynamic triaxial tests on saturated gravel soil in Nanning metro area[J]. Chinese Journal of Geotechnical Engineering, 2019, 41(1): 168−174.

[6] ZHOU Wen-quan, LENG Wu-ming, CAI De-gou, et al. Analysis on characteristics of critical dynamic stress and accumulative deformation of coarse-grained soil subgrade filling under cyclic loading[J]. Journal of Railway, 2014, 36(12): 84−89.

[7] LENG Wu-ming, ZHOU Wen-quan, NIE Ru-song, et al. Analysis of dynamic characteristics and accumulative deformation of coarse-grained soil filling of heavy-haul railway[J]. Rock and Soil Mechanics, 2016, 37(3): 728−736.

[8] FU Z, CHEN S, HAN H. Experimental investigations on the residual strain behavior of a rockfill material subjected to dynamic loading[J]. Journal of Materials in Civil Engineering, 2017, 29(5): 04016278.

[9] SUN Q D, INDRARATNA B, NIMBALKAR S. Effect of cyclic loading frequency on the permanent deformation and degradation of railway ballast[J]. Géotechnique, 2014, 64(9): 746−751.

[10] INDRARATNA B, THAKUR P K, VINOD J S. Experimental and numerical study of railway ballast behavior under cyclic loading[J]. International Journal of Geomechanics, 2010, 10(4): 136−144.

[11] CAI Yuan-qiang, ZAO Li, CAO Zhi-gang, et al. Experimental study on dynamic characteristics of unbound granular materials under cyclic loading with different frequencies[J]. Chinese Journal of Rock Mechanics and Engineering, 2017, 36(5): 1238−1246.

[12] LI Yang-bo, ZHANG Jia-sheng, ZHU Zhi-hui, et al. Study on dynamic characteristics of coarse grained soil filler in railway subgrade under stepped axial cyclic loading[J]. Journal of Railway Science and Engineering, 2019, 16(3): 620−628.

[13] LATHA G M, AM N V. Static and cyclic load response of reinforced sand through large triaxial tests[J]. Japanese Geotechnical Society Special Publication, 2016, 68(2): 2342−2346.

[14] MOAYED R Z, ALIBOLANDI M. Effect of geotextile reinforcement on cyclic undrained behavior of sand[J]. Soil Dynamics and Earthquake Engineering, 2018, 104: 395−402.

[15] WANG Jia-quan, CHANG Zhen-chao, HUANG Shi-bin, et al. Experimental analysis of dynamic characteristics of geogrid reinforced gravel soil under cyclic dynamic load[J]. Science Technology and Engineering, 2019, 19(33): 350−357.

[16] LIU J, XIAO J. Experimental study on the stability of railroad silt subgrade with increasing train speed[J]. Journal of Geotechnical and Geoenvironmental Engineering, 2010, 136(6): 833−841.

[17] HUANG Bo, DING Hao, CHEN Yun-min. Simulation of high-speed train load by dynamic triaxial tests[J]. Chinese Journal of Geotechnical Engineering, 2011, 33(2): 195−202.

[18] WANG Jia-quan, ZHANG Liang-liang, CHEN Ya-jing, et al. Mesoscopic analysis of reinforced sand triaxial test using PFC$^{3D}$[J]. Journal of Hydraulic Engineering, 2017, 8(4): 426−434, 445.

[19] BAO Cheng-gang. The principle and application of geosynthetics in engineering[M]. Beijing: China Water and Power Press, 2008: 129−131.

[20] LIU Da-peng, YANG Xiao-hua, WANG Jing, et al. Study on influence factors of gravel soil accumulative deformation under cyclic loading[J]. Journal of Railway Science and Engineering, 2014, 11(4): 68−72.

[21] WU Ting-yu, GUO Lin, CAI Yuan-qiang, et al. Deformation behavior of $K_0$-consolidated soft clay under traffic load-induced stress paths[J]. Chinese Journal of Geotechnical Engineering, 2017, 39(5): 859−867.